

# Efficient Foil Shape Optimization Using Artificial Neural Network-Based Surrogate Model with Adaptive Sampling Strategy

1<sup>st</sup> Nayma Hassan Emu

*dept. of Mechanical Engineering*  
*Bangladesh University of Engineering and Technology*  
Dhaka, Bangladesh  
naymahassanemu@gmail.com

2<sup>nd</sup> Tayyib Ahsan

*dept. of Mechanical Engineering*  
*Bangladesh University of Engineering and Technology*  
Dhaka, Bangladesh  
tayyibahsan17@gmail.com

3<sup>rd</sup> Zobair Ibn Awal

*dept. of Naval Architecture and Marine Engineering*  
*Bangladesh University of Engineering and Technology*  
Dhaka, Bangladesh  
zobair@name.buet.ac.bd

4<sup>th</sup> Minhazul Islam

*dept. of Aerospace Engineering*  
*Samuel Ginn College of Engineering, Auburn University*  
Auburn, United States  
mzi0040@auburn.edu

**Abstract**—To overcome the limitations of experimental and numerical design processes in terms of time, cost, efficiency, and uncertainty, researchers are developing optimization frameworks utilizing surrogate models based on Artificial Neural Networks (ANNs). Further enhancement of these frameworks is achieved by integrating adaptive sampling methods, which improve efficiency by reducing the number of training samples needed to reach optimal solutions. In this study, the aerodynamic shape of NACA0012 airfoil was optimized using an ANN-based surrogate model that investigated two different sampling techniques: One-Shot sampling with a Sobol sequence and Optimization-Based Adaptive sampling. The Hicks-Henne function was used to deform the shape, XFOIL was used for numerical simulations, and Sequential Least Squares Programming (SLSQP) was employed as the optimizer. Aerodynamic coefficients at the optimal points were compared for both sampling techniques. Although both strategies improved Lift and Aerodynamic Efficiency, the Optimization-Based Adaptive Sampling model found the global maximum, while the One-Shot Sampling remained at a local maximum. The Adaptive Sampling ANN model increased lift by 58.68%. Moreover, the errors of predicted optima for both models were calculated relative to XFOIL results. The Adaptive Sampling ANN model displayed superior accuracy at the optimum. However, both models performed similarly across the design space.

**Index Terms**—Artificial Neural Network, Aerodynamic Shape Optimization, Sobol Sampling, Optimization-Based Adaptive Sampling, XFOIL, Hicks-Henne Function, SLSQP

## I. INTRODUCTION

Traditional manual design methods, such as parametric analyses and cut-and-try techniques, database-matrix approaches, and other intuitive approaches, heavily rely on data and expertise. These methods are generally unsystematic, and often inefficient practices, which provide discrete designs in the design space, leaving considerable uncertainty in optimality [1]. Whereas methods like Computational Fluid Dynamics

(CFD) based Iterative Design and Analysis require a great deal of processing power which can be both time-consuming and costly. To tackle these problems, researchers have developed optimization algorithms based on surrogate models, including the kriging model [2], the support vector machine model [3], and the neural network model [4]. By eliminating the necessity of extensive numerical computations, the surrogate models have gained popularity in aerodynamic design.

Despite their popularity in aerodynamic design, there is variation in performance among these surrogate models in different conditions. Zhang et al. [5] showed that the modeling accuracy of Support Vector Machine regression model in aerodynamic prediction of small samples in wind tunnel test is poor, which is difficult to meet the needs of engineering application. Moreover, RBF neural network shallow learning prediction effect is better than Support Vector Machine regression model, but for training sets with strong nonlinearity and weak regularity, the degree of freedom of RBF neural network with single hidden layer can't meet the accuracy requirements of prediction model. They identified the Kriging model to be the best one among the three shallow learning models for aerodynamic prediction of small samples in wind tunnel test.

Nevertheless, training these surrogate models require extensive experimental or numerical data generation as well, which defeats the purpose of shifting towards surrogate model in the first place. Therefore, it makes sense to further reduce the number of training samples with an aim to reach the global optimum of an optimization problem as fast as possible. This leads the coupling of surrogate models with adaptive sampling, which iteratively improves the approximation. A more precise Optimization-Based Adaptive Sampling has been proven to be more efficient in previous studies [6], [7]. A noteworthy study is the study of Kim and Boukouvala [8].

They tested different subset selection methods over a large set of box-constrained and constrained benchmark problems with up to 30 dimensions, and their performance is compared to that of the popular interpolating surrogate modeling technique, Kriging. Their results indicated that the use of this Optimization-Based Adaptive Sampling lead to more problems solved when sampling is limited. All of their subset selection methods showed promising performance, especially for low-dimensional problems. But this is not the only sampling method that improves the efficiency of a framework.

Jiangtao et al. [9] established a new sampling method called RMSE and crowdness enhance (RCE) adaptive sampling. Their results show that RCE adaptive sampling method not only reduces the requirement for the number of samples, but also effectively improves the prediction accuracy of the surrogate model. Moreover, in 2020, Li et al. [10] proposed a new sampling method for airfoils and wings, which is based on a deep convolutional generative adversarial network (DCGAN). They trained the network to learn the underlying features among the existing airfoils and to generate sample airfoils that are notably more realistic than those generated by other sampling methods. They showed that the model can be trained using a small database of only dozens of airfoils, and synthetic airfoils of this model reserve the specific geometric features of training airfoils. In 2024, Wang et al. [11] proposed a surrogate model based on ensemble learning (Ensemble) and a hybrid sampling strategy for any surrogate model. Given the assistance of hybrid sampling, they reduced the average number of CFD calls by more than 48.2% compared to that of Non-dominated Sorting Genetic Algorithm-II (NSGA-II) and Particle Swarm Optimization (PSO).

The purpose of exploring these sampling strategies is to develop a framework that can find the global optimum value using as few samples as possible, thereby reducing computational time and cost. Contemporary research has been focused on not only developing certain surrogate based optimization frameworks but also finding strategic ways to further minimize cost and time.

In this study, an optimization framework has been developed to enhance foil efficiency by maximizing lift while constraining drag and sectional area to remain constant. The NACA0012 airfoil was chosen as the base foil for the optimization process due to its predictability and popularity in research. Surrogate models were developed using Artificial Neural Networks (ANN) to predict the aerodynamic coefficients with respect to the design variables. Furthermore, the added benefits of using Optimization-Based Adaptive Sampling as opposed to One-Shot Sampling have been investigated, focusing on reaching the global optimum with a reduced number of samples.

## II. METHODOLOGY

### A. Shape Parameterization

This study utilizes the Hicks-Henne bump function [12] to parameterize the shape of the original airfoil. This method has shown good results in airfoil parameterization with a low

number of design parameters [13]. Moreover, Hicks-Henne functions also provide sufficiently smooth geometries, along with adequate freedom in shape deformation without altering the positions of the leading and trailing edges [14]. Since the optimization is performed for a specific flow condition, the angle of attack should be kept constant. This means that the positions of the leading and trailing edges cannot be changed. Considering these requirements, the Hicks-Henne bump function has been chosen as the shape parameterization method for this study.

In this function, a linear combination of  $n$  augmented sine functions is added to the original coordinates of the airfoil in the form of a bump. With this parameterization, the upper and lower surfaces of the airfoil are deformed independently. The function can be written in this form:

$$y_{\text{mod}} = y_0 + \sum_{i=0}^n a_i \sin^{w_i} \left( \pi x \frac{\ln(0.5)}{\ln(x_i^M)} \right) \quad (1)$$

Where,  $y_0$  = initial coordinates of the upper or lower surface of the airfoil,  $y_{\text{mod}}$  = final coordinates of the upper or lower surface of the airfoil,  $n$  = number of bumps for each one of the upper or lower surfaces,  $x_i^M = x$  coordinate of the bump or  $x$  coordinate of the control point.  $w_i$  = bump width,  $a_i$  = bump intensity or coordinate's values of the control point. For this airfoil deformation process, all other parameters ( $x_i^M, w_i$ ) except for the bump intensity ( $a_i$ ) are kept fixed or unchanged. Therefore, the design variable is the bump intensity ( $a_i$ ).

In this case, four control points have been chosen for each of the upper and lower surfaces, resulting in a total of eight design variables or bump intensities ( $a_i = x_1, x_2, x_3, \dots, x_8$ ) required for this problem. The design variables are points on the airfoil surface taken at 20%, 40%, 60%, and 80% of the chord on the suction side and pressure side. A Python code was written to create the Hicks-Henne function and generate deformed foil shapes.

### B. Sampling Strategies

After defining the design variables and surrogate model type, it is crucial to determine how to vary the parameters within the design space. The sampling method significantly affects the effectiveness of the surrogate model, influencing both the outcome and the number of samples required. Sampling for surrogate models can be categorized into two types. Standard Surrogate Model Optimization (SSMO) typically uses a one-shot sampling approach, such as Latin hypercube sampling (LHS), Sobol sampling, or random sampling, where the number of computer simulations is fixed at the start of the process. In contrast, Iterative Surrogate Model Optimization (ISMO) employs sequential sampling techniques to build a sufficiently accurate surrogate using as few samples as possible.

In design optimization problems, such as aerodynamic shape optimization (ASO), it is essential to develop a surrogate model that accurately predicts the region of interest—such as minima or maxima—with high precision, using a small number of samples. Since data collection is computationally expensive and time-consuming, an incremental approach to placing

samples efficiently is preferred. As the goal of surrogate-based optimization (SBO) is to find the global optimum, points near the optima are more critical than others. Thus, building a surrogate that uniformly fits the entire design space would be inefficient given the sample constraints. Therefore, newly added data points should be chosen selectively to ensure the surrogate accurately fits the region near the optimum. This strategy effectively focuses on areas with a higher likelihood of containing the global optimum. It should be emphasized that this study aims to generate a sufficiently accurate surrogate for predicting the region of the optimum, rather than one that fits the entire design space. Consequently, the final model may have lower accuracy in regions of lesser interest but will be highly accurate around the optimum.

This study explores two different sampling techniques. One is the quasi-random, low-discrepancy sequence known as Sobol sampling, which fills the design space uniformly. The other method is an optimization-based adaptive sampling strategy, where an initial set of samples is generated using Sobol, followed by the iterative addition of a selectively chosen sample set.

1) *Sobol Sampling*: Sobol sequences [15] represent a type of quasi-random, low-discrepancy, and low-dispersion sequence. These sequences, which fall under Quasi-Monte Carlo methods, exhibit a faster convergence rate compared to standard Monte Carlo algorithms [16]. In this study, Sobol sequencing was chosen as one of the sampling methods due to its ability to evenly distribute points in space by minimizing empty regions. As previously mentioned, eight design variables were selected, representing the bump intensities of the Hicks-Henne function for the upper and lower surfaces of the airfoil. Using Python’s Quasi-Monte Carlo submodule (`scipy.stats.qmc`), samples of design variables were generated (Figure 1).

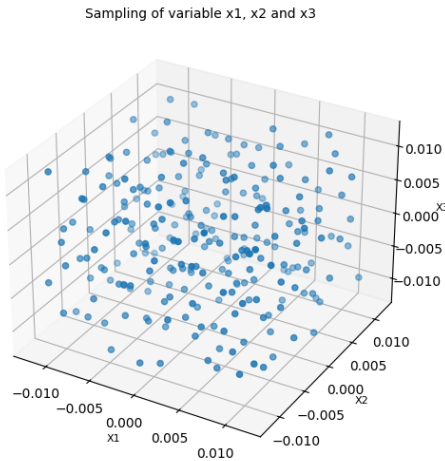


Fig. 1. Example of Sobol sampling of design variables.

2) *Optimization-Based Adaptive Sampling*: Optimization-based adaptive sampling is an iterative technique that begins by generating an initial set of samples using a space-filling

method, such as Sobol sampling. A surrogate model is then built based on these samples. Due to the limited number of initial samples, the first surrogate model usually has low accuracy. To refine the initial surrogate model, it is optimized, even in its inaccurate state, to identify potential optima. To locate both global and local optima, multiple optimizations are performed using different initial points. Once the optima are found, new sample points are generated around these regions, forming clusters near the optima. These clusters are created using Sobol sampling within smaller, defined boundaries. The surrogate model is then updated with the newly acquired samples, and the process is repeated iteratively. The procedure continues until one of the following criteria is met: (1) the solution does not improve over a consecutive set of iterations, (2) the solution shows minimal variation with different initial points, or (3) a feasible solution is reached with sufficiently low loss. Figure 2 illustrates the overall process of optimization-based adaptive sampling for an unknown function.

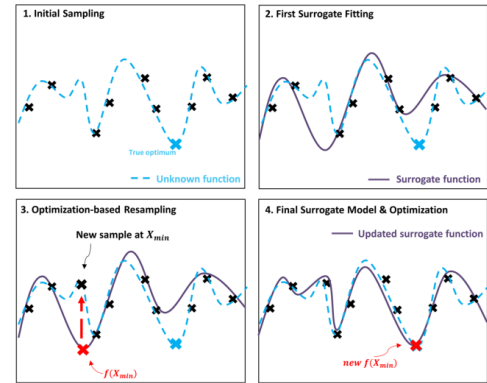


Fig. 2. Optimization-based adaptive sampling. [?]

### C. Numerical Simulation

The numerical simulation of the base airfoil NACA0012 and the deformed foils was performed using an interactive program designed for the analysis and design of subsonic isolated airfoils, called XFOIL [17]. XFOIL can be used for both viscous and inviscid analyses, as well as for airfoil design and inverse design. The inviscid formulation utilizes a linear-vorticity panel method, while to account for viscous effects, XFOIL combines the potential flow solution with boundary layer analysis [18].

In this study, the shape of the NACA0012 airfoil was optimized under fixed flow conditions. The lift and drag coefficients of the base and deformed foils were extracted from XFOIL simulations using an automated Python script. The flow conditions were:  $Re = 1 \times 10^6$ ,  $\alpha = 5^\circ$ . The viscous solution iteration limit (ITER) in XFOIL was increased to allow up to 20 Newton iterations to ensure convergence. This adjustment was made to avoid missing results and non-converging calculations with more intricate foil designs. The number of panel nodes was kept at 160.

#### D. ANN Model Training

In this research, the surrogate model was developed by implementing an ANN model structured as a Feed Forward Neural Network, where each neuron is connected to every neuron in the next layer. The input neurons represent the design variable values, and the output neurons represent the lift and drag coefficient values. The model training was implemented in Python, utilizing the TensorFlow framework, with Keras for the machine learning-specific components.

Before the training process, the data was cleaned to remove any missing values and duplicates. To improve learning performance, all inputs were normalized to fall within the range  $[-1,1]$  before the start of the training phase. The total dataset was divided into 5 folds for cross-validation. This cross-validation set was used to estimate the generalization error of the surrogate model. During the training process, the loss function was set to Mean Absolute Error (MAE), and the metrics evaluated were Mean Squared Error (MSE), Root Mean Squared Error (RMSE), and Mean Absolute Percentage Error (MAPE). The Adam optimizer was used with a learning rate of 0.01, and the tanh activation function was applied to the hidden layers. L2 regularization was implemented to prevent overfitting. The loss function values and metrics were evaluated by varying the number of neurons in the hidden layer using K-fold cross-validation. The model that produced the lowest loss was selected as the surrogate model, which is shown in Table I.

TABLE I  
TRAINING PARAMETERS FOR ANN MODEL

Input Layer	Hidden Layer	Output Layer	Regularizer	Optimizer	Learning Rate
8	$14 \times 1$	2	$L^2 : 0.01$	Adam	0.01
Loss Function	Metrics			Activation Function	Validation Set
MAE	MSE	RMSE	MAPE	Tanh	20%

#### E. Surrogate Model Optimization

Using the Python module `scipy.optimize.minimize`, the SLSQP optimizer was employed to implement the optimization of the surrogate model. Sequential Least Squares Programming (SLSQP) minimizes a function of several variables, allowing for any combination of bounds, equality, and inequality constraints. The objective of this optimization problem is to maximize the lift coefficient ( $C_L$ ) while keeping the drag coefficient ( $C_D$ ) constant and maintaining a constant area with respect to the design variables. As previously mentioned, the base airfoil is NACA0012, and the number of design variables is 8. To eliminate unrealistic airfoil shapes, the design variables are constrained to  $\pm 10\%$  of the airfoil's thickness. We restrict the boundaries of each variable to  $[-0.012, 0.012]$ . The design space lies between the regions of the green and orange curves shown in Figure 3.

Objective:  $\min(-C_L)$   
 Constraint 1:  $C_D = C_{D_{\text{original}}}$   
 Constraint 2:  $A = A_{\text{original}}$   
 Flow condition:  $Re = 1 \times 10^6$ ,  $\alpha = 5^\circ$ .

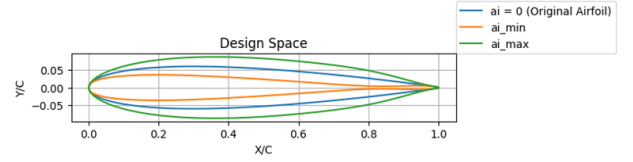


Fig. 3. Design space for optimization.

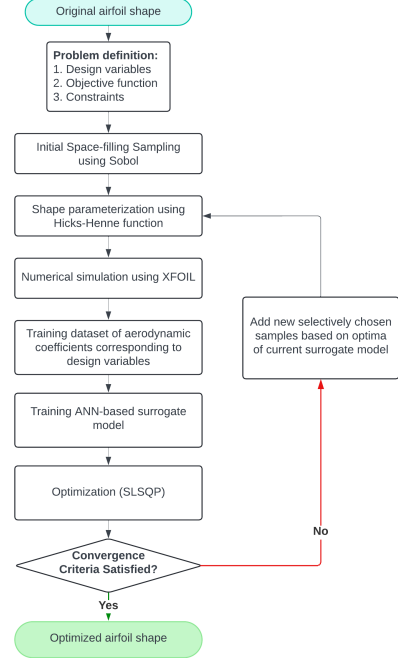


Fig. 4. Optimization Flowchart for Adaptive Sampling Method

1) *Surrogate Model Optimization with Adaptive Sampling:* In the case of the adaptive sampling method, the initial samples were generated using a low-discrepancy Sobol sequence. Using the Hicks-Henne function, the deformed foil geometry was generated based on the sample set of design variables. XFOIL simulations of the deformed foils were performed to extract the aerodynamic coefficients ( $C_L$ ,  $C_D$ ). A training dataset of  $C_L$  and  $C_D$ , corresponding to the design variables, was created. An ANN-based surrogate model was then trained. Optimization of the surrogate model was performed to find both the local and global optima. In this case, three different optimizations were carried out using three initial points, which yielded different solutions. If the convergence criteria were not met, four more points around each optimum were added using Sobol, resulting in an additional 15 points for each iteration. The new points were added to the previous sample set, and the entire process was repeated until convergence. In this paper, 128 initial points were generated using Sobol sampling, and samples were added over three iterations, leading to a total of 173 samples by the final iteration. The process flowchart of this method is illustrated in Fig. 4.

2) *Surrogate Model Optimization with One-shot Sampling:* In the one-shot sampling case, the entire optimization is

completed in a single sequence of processes. The total number of samples is generated at the initial stage using space-filling sampling methods like the Sobol sequence. Subsequently, shape parameterization, numerical simulation, dataset generation, model training, and optimization are performed sequentially. To compare with the adaptive sampling method, 173 samples were generated using Sobol sampling.

### III. RESULTS AND DISCUSSION

With the aim to locate the global optimum, while concurrently reducing the sampling requirements, an Optimization-Based Adapting Sampling is used. Fig. 5 illustrates the Lift

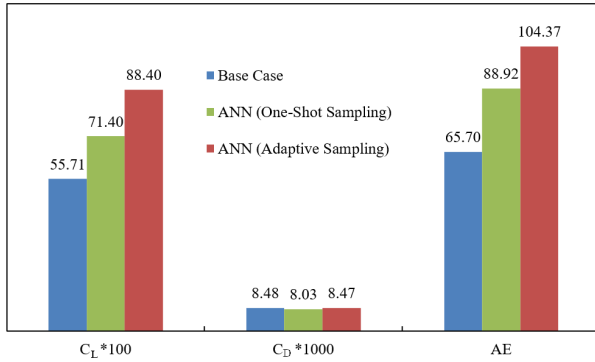


Fig. 5. Comparison of the aerodynamic coefficients of optimum for different sampling techniques

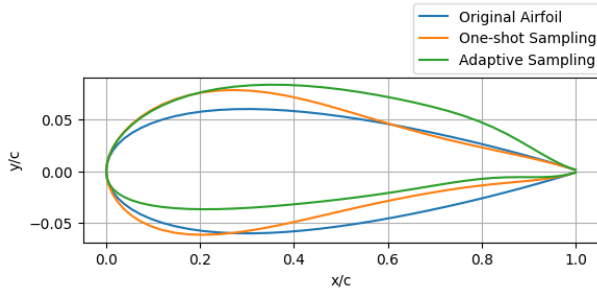


Fig. 6. Geometries of baseline and optimal airfoil

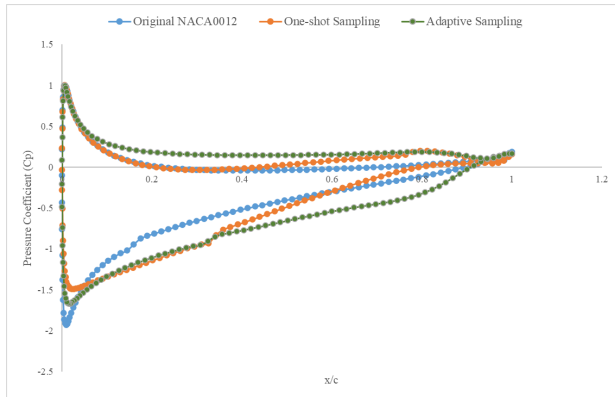


Fig. 7. Comparison of pressure coefficients between baseline and optimal airfoil

coefficient ( $C_L$ ), Drag coefficient ( $C_D$ ) and Aerodynamic Efficiency ( $AE = C_L/C_D$ ) of the Base Case, ANN model with one-shot sampling and ANN model with adaptive sampling for the final sampling size of 173. Here, the ANN model with adaptive sampling, leads to an optimized foil shape that exhibits 58.68% more lift relative to the base case, whereas, the ANN with one-shot sampling method leads to 28.16% more lift compared to the base case. These values indicate that for the same number of samples, the adaptive sampling method enabled the optimizer to reach a global optimum more efficiently, while the one-shot sampling model is still stuck at a local optimum. As the drag was constrained to be constant, the  $C_D$  bars are almost equal for all cases. The slight reduction in the one-shot sampling model indicates its proclivity to underestimate the drag. Moreover, due to the drag constraint, the percentage of increase in Aerodynamic Efficiencies is almost analogous to the percentages of Lift coefficients increase. The deformed geometries are illustrated in Fig. 6. If we analyze the XFOIL results displayed in Fig. 7, the increased lift can be explained by a decrease in pressure on the suction side, accompanied by an increase in pressure along the lower surface of the foil.

Nevertheless, reaching a global optimum is only half the optimization problem. In order for the optimization method to be useful, the surrogate model prediction at the optimum point has to be accurate, i.e., it has to mimic the true value closely enough so that the predicted optimum value is sufficiently reliable. Fig. 8 depicts the percentage of error of the predicted optimum relative to the XFOIL calculated result. If we consider the blue bar that represents the  $C_D$  of the optimum value for the adaptive sampling model, we can see it started off at 22.5%, steadily decreasing through the iterations to around 18%, then around 7%, and nearly diminishing at the end. The error for Lift coefficients of the adaptive sampling model represented by the brown bar, increases at first to 9.75% from 5.33%, however, decreases to 8.47%, then suddenly drops to a little under 2%. For both  $C_D$  and  $C_L$ , the adaptive sampling method decreased the percentage of error significantly at the end of the iterations. With the increased sample size, the one-shot sampling method also decreased the percentage of error

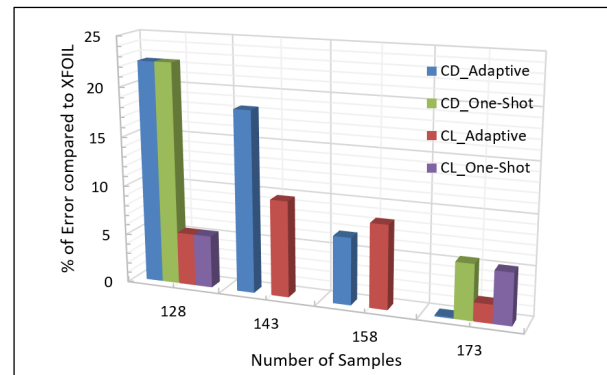


Fig. 8. Percentage of error of predicted optimum compared to XFOIL

TABLE II  
PERFORMANCE METRICS

Iteration	ANN with Adaptive Sampling	Sample count	MAE	MSE	RMSE	MAPE
0	Sobol (one-shot)	128	1.21E-02	3.30E-04	1.82E-02	1.27E+01
1	Sobol + selective (Adaptive)	143	1.27E-02	4.94E-04	2.22E-02	4.57E+00
2	Sobol + selective (Adaptive)	158	1.24E-02	3.52E-04	1.87E-02	6.79E+00
3	Sobol + selective (Adaptive)	173	1.26E-02	3.89E-04	1.97E-02	4.74E+00
Case	ANN with One-Shot Sampling	Sample count	MAE	MSE	RMSE	MAPE
1	Sobol (one-shot)	173	1.35E-02	5.78E-04	2.40E-02	5.42E+00

considerably, yet, not as significantly as the adaptive sampling method. The percentage of error for  $C_D$  decreased down to 5.61%, while the error for  $C_L$  remained fairly the same. This goes to show that the Adaptive Sampling method predicted the optimum value more accurately, compared to the One-Shot Sampling method.

Despite the added accuracy at the optimum point and a reduced number of required samples, the ANN model trained with adaptive sampling method performs similarly to the ANN model trained with one-shot sampling all over the design space. If we consider the errors of iteration-3 and case-1 from Table II, we can observe that the MAE, MSE, RMSE and MAPE of both models are fairly similar.

#### IV. CONCLUSIONS

This study explores machine learning techniques to tackle design optimization problems, which, in practical cases, can be used to significantly reduce the computational cost and time of engineering design. In this paper, an optimization framework has been developed to enhance foil efficiency by maximizing lift while constraining drag and sectional area to remain constant. Moreover, two sampling strategies were investigated: One-Shot Sampling and Optimization-Based Adaptive Sampling. Both sampling strategies resulted in a significant increase in lift and aerodynamic efficiency. However, for the same number of samples, the Optimization-Based Adaptive Sampling was able to find the global maximum, whereas the One-Shot Sampling model remained adhered to a local maximum. The ANN model with Adaptive Sampling led to an optimized foil shape that exhibits 58.68% more lift relative to the base case. This selective sampling method considerably increased the accuracy of the surrogate model at the optimum point. In contrast, the One-Shot Sampling did not achieve the same level of accuracy at the optimum point. However, both models showed similar performance across the entire design space.

#### REFERENCES

[1] O. Baysal, "Aerodynamic shape optimization: Methods and applications," *SAE Transactions*, vol. 108, pp. 794–802, 1999. [Online]. Available: <http://www.jstor.org/stable/44729475>

[2] S. Jeong, M. Murayama, and K. Yamamoto, "Efficient optimization design method using kriging model," *Journal of Aircraft*, vol. 42, no. 2, pp. 413–420, 2005.

[3] Q. Wang, W. Qian, and K. He, "Unsteady aerodynamic modeling at high angles of attack using support vector machines," *Chinese Journal of Aeronautics*, vol. 28, no. 3, pp. 659–668, 2015. [Online]. Available: <https://www.sciencedirect.com/science/article/pii/S1000936115000552>

[4] D. F. Kurtulus, "Ability to forecast unsteady aerodynamic forces of flapping airfoils by artificial neural network," *Neural Computing and Applications*, vol. 18, pp. 359–368, 2009.

[5] C. Zhang, Z. Wei, J. Wu, G. Li, and K. Zhu, "Application of shallow learning in aerodynamic prediction of wind tunnel test," in *2023 2nd International Conference on Machine Learning, Cloud Computing and Intelligent Mining (MLCCIM)*, 2023, pp. 6–17.

[6] A. Cozad, N. V. Sahinidis, and D. C. Miller, "A combined first-principles and data-driven approach to model building," *Computers Chemical Engineering*, vol. 73, pp. 116–127, 2015. [Online]. Available: <https://www.sciencedirect.com/science/article/pii/S0098135414003287>

[7] D. R. Jones, M. Schonlau, and W. J. Welch, "Efficient global optimization of expensive black-box functions," *Journal of Global optimization*, vol. 13, pp. 455–492, 1998.

[8] S. H. Kim and F. Boukouvala, "Machine learning-based surrogate modeling for data-driven optimization: a comparison of subset selection for regression techniques," *Optimization Letters*, vol. 14, no. 4, pp. 989–1010, 2020.

[9] J. Huang, Z. Gao, Z. Zhou, and K. Zhao, "An improved adaptive sampling and experiment design method for aerodynamic optimization," *Chinese Journal of Aeronautics*, vol. 28, no. 5, pp. 1391–1399, 2015. [Online]. Available: <https://www.sciencedirect.com/science/article/pii/S1000936115001570>

[10] J. Li, M. Zhang, J. Martins, and C. Shu, "Efficient aerodynamic shape optimization with deep-learning-based geometric filtering," *AIAA Journal*, vol. 58, pp. 1–17, 07 2020.

[11] S. Wang, Q. Xu, and N. Wei, "Airfoil aerodynamic optimization design using ensemble learning surrogate model," *Journal of Aerospace Engineering*, vol. 37, no. 6, p. 04024093, 2024. [Online]. Available: <https://ascelibrary.org/doi/abs/10.1061/JAEEZS.ASENG-5410>

[12] R. M. Hicks and P. A. Henne, "Wing design by numerical optimization," *Journal of Aircraft*, vol. 15, no. 7, pp. 407–412, 1978. [Online]. Available: <https://doi.org/10.2514/3.58379>

[13] P. Castonguay and S. Nadarajah, *Effect of Shape Parameterization on Aerodynamic Shape Optimization*. [Online]. Available: <https://arc.aiaa.org/doi/abs/10.2514/6.2007-59>

[14] M. Zanichelli, "Shape optimisation of airfoils by machine learning-based surrogate models - master's thesis - marco zanichelli - politecnico di milano," 12 2021.

[15] I. M. Sobol', "Distribution of points in a cube and the approximate evaluation of integrals (in Russian)," *Zhurnal Vychislitel'noi Matematiki i Matematicheskoi Fiziki*, vol. 7, pp. 784–802, 1967.

[16] F. Y. Kuo, W. T. M. Dunsmuir, I. H. Sloan, M. P. Wand, and R. S. Womersley, "Quasi-monte carlo for highly structured generalised response models," *Methodology and Computing in Applied Probability*, vol. 10, no. 2, pp. 239–275, Jun. 2008. [Online]. Available: <https://doi.org/10.1007/s11009-007-9045-3>

[17] M. Drela, "Xfoil: An analysis and design system for low reynolds number airfoils," vol. 54, 06 1989.

[18] M. Drela and M. GILES, "Viscous-inviscid analysis of transonic and low reynolds number airfoils," *Aiaa Journal - AIAA J*, vol. 25, pp. 1347–1355, 10 1987.